

A Monoclinic Post-Stishovite Polymorph of Silica in the Shergotty Meteorite

Ahmed El Goresy,^{1*} Leonid Dubrovinsky,² Thomas G. Sharp,³
Surendra K. Saxena,² Ming Chen⁴

A post-stishovite phase of silica was identified in the Shergotty meteorite by x-ray diffraction and field emission scanning electron microscopy. The diffraction pattern revealed a monoclinic lattice, similar to the baddeleyite-structured polymorph with the cell parameters $a = 4.375(1)$ angstroms, $b = 4.584(1)$ angstroms, $c = 4.708(1)$ angstroms, $\beta = 99.97(3)$, $\rho = 4.30(2)$ grams per cubic centimeter, where the numbers in parentheses are the maximum deviations. Transmission electron microscopy investigations indicate the presence of the α -lead dioxide-like polymorph, stishovite, and secondary cristobalite in the same silica grain. The mixture of high-density polymorphs suggests that several post-stishovite phases were formed during the shock event on the Shergotty parent body.

Silica (SiO_2) is one of the primary components of Earth. Based on the chondritic model, SiO_2 makes up 50 weight percent (wt %) of Earth's bulk. This raises the question of the presence of free silica polymorphs in Earth's mantle. Although it is generally accepted that the SiO_2 component of Earth's lower mantle occurs as $(\text{Mg,Fe})\text{SiO}_3$ -perovskite, experimental evidence for the breakdown of perovskite at about 80 GPa (1, 2) suggests that free silica may exist in the lower mantle. Silicon is tetrahedrally coordinated by oxygen in low-pressure SiO_2 polymorphs quartz, tridymite, and cristobalite, and in its high-pressure polymorph, coesite. It is coordinated by six oxygens in the high-pressure SiO_2 polymorph stishovite. The synthesis of stishovite (3) and its subsequent discovery in naturally shocked rocks (4, 5) has ignited the interest in shock metamorphism by providing an index mineral, in addition to coesite, that can be used as proof of exogenic metamorphic events (4–8). Possible polymorphs of silica denser than stishovite (post-stishovite) are also important for understanding the dynamic history of shocked rocks in terrestrial impact craters because they could serve as indicators of higher shock pressure. Additional constraints on the shock pressures experienced by meteorites are important to unravel the impact records of asteroids and planets in the early history of the solar system.

High-pressure diamond anvil cell experiments and theoretical calculations revealed that SiO_2 undergoes several phase transitions

to post-stishovite polymorphs above 48 GPa (9–12). At pressures above 48 GPa, stishovite inverts to the CaCl_2 -structured polymorph (space group $Pnmm$) (9, 10). This phase transition is displacive. At pressures of 70 to 85 GPa, the CaCl_2 structure transforms to an α - PbO_2 -like structure, which, like the stishovite or CaCl_2 modification, contains silicon in distorted octahedra, but with kinked chains of SiO_6 octahedra (12, 13). In situ diamond anvil cell experiments at high temperature revealed that an α - PbO_2 -like structure (space group $Pbcn$ or $Pnc2$) could stably exist above 70 GPa (12, 14). Theoretical calculations of the SiO_2 phase stability at high pressure and room temperature indicate that the α - PbO_2 -like silica (space group $Pbcn$) is stable above 85 GPa (13). Crystal chemical analysis, theoretical calculations (11, 12, 15, 16), and a comparison with structural analogues [titanium dioxide, for example (17)] suggest that the α - PbO_2 -like silica is related to the baddeleyite structure (ZrO_2), in which the silicon cation is seven-coordinated by oxygen.

Silica grains in Shergotty mostly occur as large (150 to 900 μm) wedge-shaped grains typical of β -tridymite morphology, but not of quartz (Fig. 1A) (18–20). They are either enclosed in clinopyroxene or occur between clinopyroxene, mesostasis, and maskelynite. Each grain is surrounded by pervasive radiating cracks that initiate at the surfaces of the silica grains and penetrate deep (up to 600 μm) into the Shergotty matrix (Fig. 1A) (18–20). The radiating cracks are similar to those reported from ultra-high pressure metamorphic rocks around coesite grains (21) and are indicative of a large volume increase after decompression. Every silica grain (Fig. 1B) consists of mosaics of domains (10 to 60 μm in diameter), each displaying orthogonal sets of lamellae that have different brightness in back-scattered electron imaging (BSE) mode

in the field emission scanning electron microscopy (FESEM) (Fig. 1B). Numerous domains depict areas barren of or poor in lamellar intergrowth (Fig. 1B). Electron microprobe analyses with a defocused beam on the widest lamellae and on areas poor in lamellae showed almost pure SiO_2 with minor concentrations in Na_2O (0.40 wt %) and Al_2O_3 (1.14 wt %).

A 0.9-mm disc containing a large SiO_2 (420- μm -long and 80- μm -wide) grain with lamellar textures and areas poor in lamellar intergrowth (Fig. 1B) was cored out with a high-precision diamond microdrill for successive x-ray (22) and transmission electron microscopy (TEM) investigation. This grain was exposed on upper and lower surfaces of the cored disc. This is preferable for in situ x-ray investigations because there is little danger of additional phases contributing x-ray lines to the data set (23). The major constituents of the sample were an augite-pigeonite intergrowth, titanomagnetite, maskelynite, and a SiO_2 phase (Table 1) (24). The augite-pigeonite assemblage identified by x-ray is in good agreement with previous studies (25). All crystalline phases demonstrated a high degree of preferred orientation and broadening of the x-ray reflections.

The silica grain contains some amount of amorphous material that produces a broad halo where 2θ is between 8° and 12° . We collected a total of 18 reflections from the SiO_2 grain (Table 1 and Fig. 2) (26). Some of the reflections [(2.974(6) Å, 2.023(4) Å, 1.950(8) Å, 1.568(5) Å; where the numbers in parentheses are maximum deviations] could belong to stishovite, but most of the reflections could not be assigned to any known silica polymorph. All observed reflections [except a small broad reflection at 2.639(6)] could be indexed in terms of a monoclinic lattice with the cell parameters $a = 4.375(1)$ Å, $b = 4.584(1)$ Å, $c = 4.708(1)$ Å, $\beta = 99.97(3)$, and $\rho = 4.30(2)$ g/cm^3 . The calculated density of this phase is higher than the density of stishovite ($\rho = 4.28$ g/cm^3 , Powder Diffraction File (PDF) no. 451374). The lattice parameters for the new phase are related to those of the baddeleyite-type structures. Moreover, 16 of the 18 observed reflections from the silica grain can be indexed with the baddeleyite-type structure. Exceptions are the weak unindexed reflection at 2.639(6) and the reflection at 2.974(6). The latter reflection corresponds to the (110) reflection of stishovite (100% intensity reflection of stishovite), whereas the former fits the most intense (111) reflection of the new orthorhombic post-stishovite phase (27, 28). The most intense reflections of the new monoclinic silica phase (4.309, 2.767, 2.459, 2.318, and 2.023 Å) cannot be explained as a mixture of stishovite and the α - PbO_2 phase. Although quantitative analysis of the intensities of reflections of the new silica phase is

¹Max-Planck-Institut für Chemie, J.-Becher-Weg 27, D-55128 Mainz, Germany. ²Theoretical Geochemistry Program, Institute of Earth Sciences, Uppsala University, S-75236, Uppsala, Sweden. ³Department of Geology, Arizona State University, Tempe, AZ 85287, USA. ⁴Guangzhou Institute of Geochemistry, Academia Sinica, Guangzhou 510640, China.

*To whom correspondence should be addressed. E-mail: goresy@mpch-mainz.mpg.de

subject to errors due to the strong preferred orientation and the broad diffusion halo, the calculated intensities for baddeleyite-structured SiO₂ polymorph are similar to the observed ones (Table 1 and Fig. 2). The monoclinic phase is metastable and is sensitive to x-ray irradiation damage. Using even a relatively weak x-ray beam (produced by in-house rotating anode generator), we observed a reduction in the intensities of the reflections and an increase of the intensities of the diffuse halo during successive pattern collecting in 12-hour periods.

Transmission electron microscopy was performed on the same SiO₂ grain that was used for x-ray diffraction studies (29). In bright-field TEM images, the SiO₂ grain shows several distinct textures. Much of the SiO₂ depicts intergrowths of crystalline and amorphous lamellae (Fig. 3A). The amorphous lamellae are up to 0.5- μ m wide. These relatively coarse lamellar intergrowths are probably what was observed in the FESEM images. The crystalline lamellae are cut by numerous amorphous veins that are tens of nanometers wide (27, 28). Selected area electron diffraction (SAED) patterns of the crystalline lamellae are consistent with the orthorhombic polymorph described recently (28). In addition, intergrowths of crystalline and amorphous material occur with two orthogonal

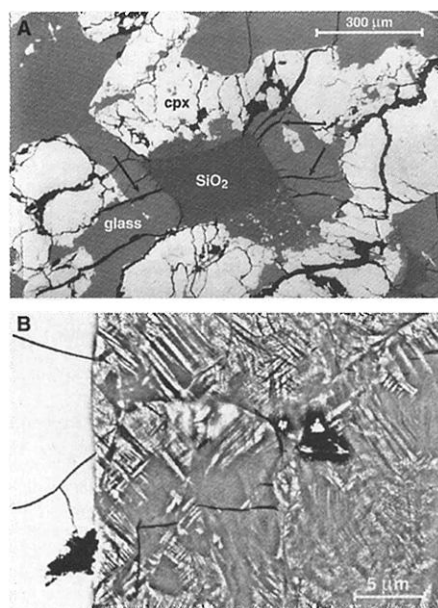


Fig. 1. BSE-mode SEM images of SiO₂ and other coexisting silicates in Shergotty. (A) A wedge-shaped silica occurring with maskelynite (glass) and clinopyroxene (cpx). The silica grain is surrounded by pervasive radiating cracks (arrows) that initiate at its surfaces and penetrate deep (up to 600 μ m) in the Shergotty matrix. It depicts concave surfaces at the top and left-hand sides demonstrating high degree of deformation. (B) High magnification FESEM of a portion of a silica grain depicting a smooth area along with orthogonal intergrowth of the post-stishovite orthorhombic phase (28) and dense SiO₂ glass.

sets of crystalline SiO₂ that are 10- to 20-nm wide (Fig. 3B). SAED patterns from these intergrowths show that the crystalline material is a mixture of stishovite, viewed along [001], and cubic cristobalite, viewed along $\langle 110 \rangle$ (Fig. 3B). Much of the SiO₂ consists of fine mixtures of crystalline and amorphous material that has been difficult to characterize. Because of sensitivity to irradiation damage, it was not possible to collect sufficient electron diffraction data to identify the crystalline material in these intergrowths. None of the electron diffraction data was consistent with the monoclinic baddeleyite-like structure identified with x-ray diffraction.

The fact that the monoclinic baddeleyite-like structure was not encountered during TEM may be the result of high instability during sample preparation for TEM. On the basis of the sensitivity of the SiO₂ polymorphs to electron, x-ray, and laser radiation (27, 28), it is possible that the unstable SiO₂ polymorphs

continue to transform to more stable low-pressure forms or vitrify during ion milling and electron irradiation. Although the same SiO₂ grain was characterized by x-ray diffraction (XRD) and TEM, the material investigated by XRD may not have been examined by TEM.

The presence of multiple SiO₂ phases is consistent with the complexity of post-stishovite structures that have been investigated experimentally and theoretically (9–13, 30). Although the shock-induced parental polymorph of the monoclinic phase and the reasons for its formation instead of the expected α -PbO₂ structured phases (9–13) are unknown, we can speculate that small amounts of impurities (such as Na₂O and Al₂O₃) and heterogeneous stress distribution in shock-wave compressed material could be factors that preserve the monoclinic phase from destruction. The presence of the monoclinic baddeleyite-like and orthorhombic α -PbO₂-

Fig. 2. Diffraction pattern obtained from areas as shown in Fig. 1B in the SiO₂ investigated. Fifteen diffraction lines are indexed in the monoclinic baddeleyite-like structure. The remaining two peaks belong to the orthorhombic α -PbO₂ polymorph (Ort) and stishovite (St), respectively (Table 1).

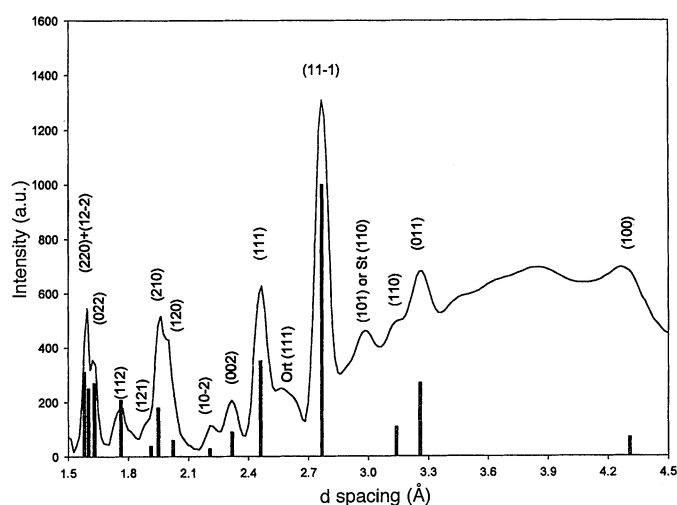
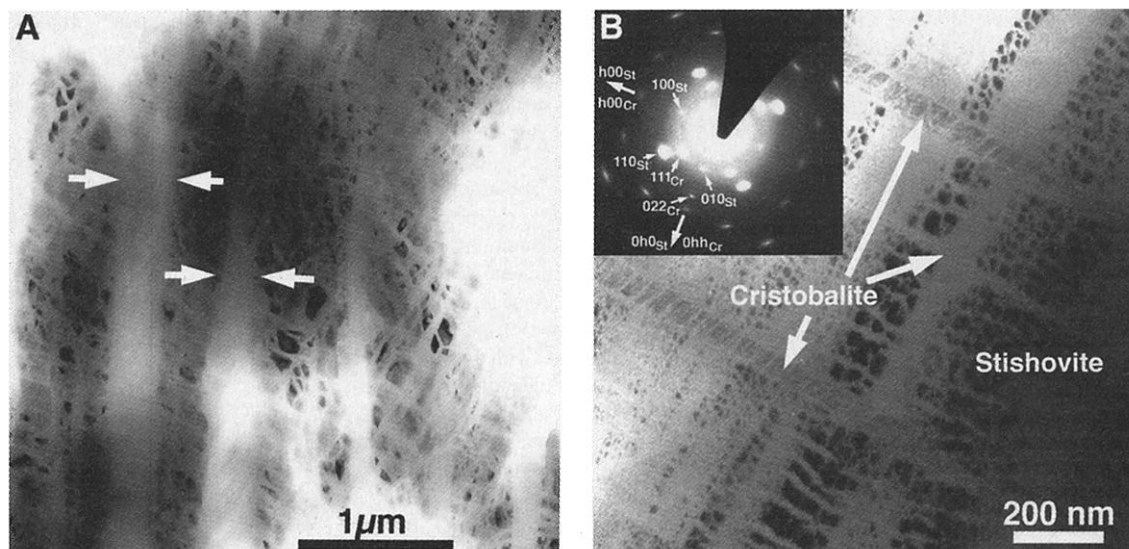


Table 1. Indexed peaks of the x-ray diffraction pattern and Miller indices collected from the silica grain in the Shergotty meteorite.

$d_{\text{obs.}}$, Å	$d_{\text{calc.}}$, Å*	$I_{\text{obs.}}$, %	$I_{\text{calc.}}$, %†	h	k	l
4.309(4)	4.3087	10	7	1	0	0
3.260(5)	3.2587	22	27	0	1	1
3.139(4)	3.1394	6	11	1	1	0
2.974(6)‡						
2.767(3)	2.7667	100	100	1	1	-1
2.639(6)		6				
2.459(8)	2.4595	31	35	1	1	1
2.318(3)	2.3183	11	9	0	0	2
2.207(4)	2.2073	8	3	1	0	-2
2.023(4)	2.0234	14	2	1	2	0
1.950(8)	1.9497	26	11	2	1	0
1.913(9)	1.9125	4	14	1	2	1
1.762(7)	1.7617	12	21	1	1	2
1.629(4)	1.6299	24	27	0	2	2
1.591(3)	1.5898	19	25	1	2	-2
1.568(5)	1.5697	18	31	2	2	0
1.458(5)	1.4573	16	14	2	0	2
1.355(6)	1.3532	8	13	1	3	1

* $a = 4.375(1)$, $b = 4.584(1)$, $c = 4.708(1)$, $\beta = 99.97(3)$, $\rho = 4.30(2)$ g/cm³. †Intensities are calculated with lattice parameters given above and coordinates of atoms for baddeleyite structure (32). ‡This reflection corresponds to the 110 reflection of stishovite (100% intensity reflection of stishovite).

Fig. 3. Bright-field TEM images of three distinct SiO₂ microstructures. A dense orthorhombic polymorph (A) coexists with large (up to 0.5 μm) vertical lamellae of amorphous SiO₂ (between arcs) and is also cut by many smaller amorphous veins that are inclined in the image. In all of these images, crystalline phases are strongly diffracting and appear dark relative to the coexisting amorphous SiO₂. (B) Stishovite (St), which appears as dark scaly material in a matrix of amorphous SiO₂, is topotaxially intergrown with lamellae of cubic cristobalite (Cr). The SAED pattern of the superimposed stishovite [001] and cristobalite <0-11> zone axes illustrates the crystallographic relation between the two phases: (h00)St || (h00)Cr and (h0h)St || (0hh)Cr. The forbidden stishovite reflections, h00, where h is odd, appear as a result of dynamic diffraction effects.



like SiO₂ polymorphs, which are possible quench products from other post-stishovite phases, indicates that Shergotty experienced higher pressures than the 29 ± 1 GPa value estimated by (31). The pressure range of 70 to 85 GPa, required for the stability of baddeleyite-like or α-PbO₂-like structures, is too high because such high pressures would have induced extensive melting in Shergotty.

The equilibrium phase boundary between the CaCl₂-structure and baddeleyite-like or α-PbO₂-like SiO₂ may not represent the reactions that took place in Shergotty. Because the precursor SiO₂ mineral was probably tridymite, the phase transformations of interest involved metastable equilibria between tridymite and post-stishovite SiO₂ phases (14). Although the pressures of these metastable boundaries are unknown, they may be well below the 70 to 85 GPa of CaCl₂-baddeleyite type or the CaCl₂-α-PbO₂ type boundary. Recent diamond anvil cell experiments on cristobalite or tridymite indicate that the α-PbO₂-like structure (space group Pnc2) could be obtained at pressures from 40 GPa up to 95 GPa (14). However, its stability at pressures higher than 95 GPa has not been experimentally explored. The complex mixture of high-density phases suggests that several metastable reactions took place during the impact event. It is necessary to investigate the SiO₂ phase transformations that occur upon quenching to better understand the transition paths upon decompression. Our findings, and those of (28), do not provide evidence of one structure being more stable than the other.

References and Notes

1. S. K. Saxena et al., *Science* **274**, 1357 (1996)
2. S. K. Saxena, L. S. Dubrovinsky, P. Lazor, J. Hu, *Eur. J. Mineral.* **10**, 1275 (1998).
3. S. M. Stishov and S. V. Popova, *Geokhimiya* **10**, 923 (1961).

4. E. C. T. Chao, J. J. Fahey, J. Littler, D. J. Milton, *J. Geophys. Res.* **67**, 419 (1962).
5. E. C. T. Chao, *Science* **156**, 192 (1967).
6. _____ and P. H. Abelson, Eds., *Research in Geochemistry* (Wiley & Sons, New York, 1967), vol. 2, p. 204.
7. E. C. T. Chao, B. M. French, N. M. Short, Eds., *Shock Metamorphism of Natural Materials*, Greenbelt, MD (Mono Book Co., Baltimore, 1968).
8. D. Stöffler, *Fortschr. Mineral.* **51**, 256 (1974).
9. R. Hemley, C. T. Prewitt, K. J. Kingma, *Rev. Mineral.* **29**, 41 (1994).
10. J. Kingma, R. E. Cohen, R. J. Hemley, H.-K. Mao, *Nature* **374**, 243 (1995).
11. A. B. Belonoshko, L. S. Dubrovinsky, N. A. Dubrovinsky, *Am. Mineral.* **81**, 785 (1996).
12. L. S. Dubrovinsky et al., *Nature* **388**, 362 (1997).
13. D. M. Teter, R. J. Hemley, G. Kresse, J. Hafner, *Phys. Rev. Lett.* **80**, 2145 (1998).
14. L. S. Dubrovinsky and S. K. Saxena, *Phys. Rev. Letters*, in preparation; *Phys. Chem. Minerals*, in preparation.
15. L. S. Dubrovinsky, A. Belonoshko, N. A. Dubrovinsky, S. K. Saxena, *High Pressure Sci. Technol.* **1996**, 921 (1996)
16. J. M. Léger, J. Haines, B. Blanzat, *J. Mater. Sci. Lett.* **13**, 1688 (1994)
17. J. S. Olsen, L. Gerward, J. Z. Jiang, *J. Phys. Chem. Solids* **60**, 229 (1999)
18. A. El Goresy, B. Wopencka, M. Chen, G. Kurat, *Meteoritics* **32**, A38 (1997).
19. T. G. Sharp, A. El Goresy, L. Dubrovinsky, M. Chen, *Meteoritics* **33**, A144 (1998).
20. A. El Goresy, L. Dubrovinsky, S. Saxena, T. G. Sharp, *Meteoritics* **33**, A45 (1998).
21. Ph. Gillet, J. Ingrin, C. Chopin, *Earth Planet. Sci. Lett.* **70**, 426 (1984).
22. The x-ray facility used in this study includes a rotating anode generator (18 kW), capillary collimating system, and a charge-coupled device (CCD) area detector. The radiation from the rotating anode with a molybdenum target is filtered by a zirconium foil so that the intensity of Kβ is 1% of that of Kα. The beam of initial size 1 × 0.5 mm is collimated to 0.1 mm diameter with the capillary system. A special collimator is used to reduce the size of the x-ray spot to 40 μm full width at half maximum (FWHM). The diffracted x-rays were collected on a 512 × 512 pixel area detector. Data were acquired at different fixed 2θ settings of 15, 25, and 30 (corresponding to the fixed positions of the detector) and a sample-to-detector distance of 210 mm. Time of collection in different points varied from 15 min to 12 hours. Settings of the detector were carefully calibrated

- with three external independent standards (W, MgO, and Al₂O₃) at each position of the detector.
23. The sample disc was mounted on a 0.8-mm hole in a larger steel disc that was loaded onto the goniometer stage for the x-ray studies.
24. The sample was first scanned with 25-μm mesh to identify the major phases in the sample.
25. W. F. Müller, *Geochim. Cosmochim. Acta* **57**, 4311 (1993).
26. Within the 420-μm-long and 80-μm-wide silica grain, four distinct points were investigated and no distinguishable differences have been found. To partially overcome the problems of preferred orientation and make the relative intensities of the reflections more representative of a powder x-ray pattern, the sample plate was rotated on 30° from the initial position normal to x-ray beam with a step of 1° in w-axis during data collection. Positions of the lines obtained as the average over all collected spectra. The position of the finely collimated x-ray beam penetrating through the silica grain was continuously monitored on a screen with a CCD camera. We made efforts to include smooth areas as shown in Fig. 1B within the four areas irradiated by the x-ray beam.
27. A. El Goresy, T. G. Sharp, M. Chen, B. Wopenka, *Lunar Planet. Sci. Conf. XXIX*, 1707 (1998)
28. T. G. Sharp, A. El Goresy, B. Wopenka, M. Chen, *Science*, **284**, 1511 (1999).
29. The sample was thinned by Ar ion bombardment with a Gatan Duomill 600 (Gatan Inc., Pleasanton, CA). To preserve the highly metastable SiO₂, we milled the ions with a liquid-nitrogen cooled sample holder and with a 4-kV accelerating potential. The sample was lightly coated with amorphous carbon to prevent charging in the electron beam. Samples were investigated with a Philips CM200-FEG (FEI Co., Eindhoven, Netherlands), a 200 kV microscope equipped with a field emission gun (FEG). To minimize irradiation damage during characterization, we collected data on a slow-scan CCD camera while using low electron doses.
30. B. B. Karki, M. C. Warren, G. J. Ackland, J. Crain, *Phys. Rev. B* **55**, 3465 (1997).
31. D. Stöffler et al., *Geochim. Cosmochim. Acta* **50**, 889 (1986).
32. J. D. McCullough and K. N. Trueblood, *Acta Crystallogr.* **12**, 507 (1959).
33. M.C. is supported by National Science Foundation of China (grant 49825132) and a Deutsche Forschungsgemeinschaft (grant Go 315/15-1). Two anonymous reviewers helped in substantially improving the manuscript.

7 January 2000; accepted 12 April 2000